Indian Journal of Engineering & Materials Sciences
Vol. 27, April 2020, pp. 396-403

Unsteady flow of CNT-water nanofluid past a stretching sheet with slip effect

Santosh Chaudhary*

Department of Mathematics, Malaviya National Institute of Technology, Jaipur 302017, India

Received: 05 September 2019; Accepted: 15 November 2019

In this analysis, an unsteady flow over a stretching plate with slip effect in CNT-water nanofluid has been examined. A set of ordinary differential equations have been obtained by applying the convenient similarity variables. Perturbation technique has been used to find numerical solutions of the study by applying Runge-Kutta fourth order scheme. Plots of velocity and temperature distributions for physical parameters such as velocity slip parameter, solid volume fraction, unsteadiness parameter and thermal slip parameter have been given via graphs, whereas numerical values of local skin friction coefficient and local Nusselt number have been presented in tabular form. Comparison with earlier published results specified that Runge-Kutta method of order four is applicable to solve this problem.

Keywords: Unsteady flow, Nanofluid, Stretching sheet, Slip effect

1 Introduction

Unsteady flows appear in natural cases like flow due to fins of fish and flapping wings of birds, and pulsating flow in arteries. The fluid flows with unsteady nature have been attracting the researchers in the past several years. Unsteady impacts emerge either due to non-uniformities or fluctuations in the surrounding fluid or due to self induced by the body. Studies on boundary layer flow with unsteady condition have been considered by Elbashbeshy and Bazid[1], Liao[2], Jat and Chaudhary[3], and Hayat and Nawaz[4]. Further, Rashad[5] determined the impacts of thermal radiation and variable viscosity on unsteady flow in the presence of magnetic field. Some recent developments with unsteady condition have been analyzed by Khan and Azam[6], Chaudhary and Choudhary[7], Dholey[8] and Moshkin *et al.*[9].

Nanofluid is a nanotechnology based fluid, which is created to improve the performance of ordinary fluids by the suspension of the nano solid particles with the diameter size 1 to 100 nm. This kind of fluid has higher single-phase heat transfer coefficient and the thermal conductivity than the conventional fluids. Nanofluids have significant impacts on the several industrial divisions due to the reason of developing features of thermal conductivity. These fluids include some applications like cooling of nuclear reactors, production of energy, power generation, cancer therapy and thermal insulation. Initially, Choi[10] had created the term nanofluid, who claimed that a suspension of nano metal particles can increase the thermal properties of the base fluids. A numerical study of nanofluid flow between parallel plates is investigated by Sheikholeslami and Ganji[11]. After that numerous researchers such as Chen *et al.*[12], Sheikholeslami and Rokni[13], Ahmed and Nadeem[14], Chaudhary and Kanika[15], and Uddin *et al.*[16] contributed for the nanofluid flow along with different configurations.

Study on stretching sheet has been initiated since last decade because this sheet is commonly created. To control the drag and heat flux for a desirable condition of the product, the stretching of a plate creates motion in the fluid parallel to the plate. Fluid flow past a stretching surface has various applications in the field of manufacturing and industrial. Some examples of applications are drawing of wire, metal spinning, extrusion of polymer and metal, hot rolling, fine-fiber mattes and thermal processing of sheets. The fluid flow past a stretchable plate has been discussed numerically by Ishak *et al.*[17]. Afterward, Tamizharasi and Kumaran[18], Chaudhary *et al.*[19] and Babu and Sandeep[20] highlighted the influence of stretching surface on fluid flow along with various considerations. Recently, several authors, namely, Liu and Liu[21] and Hamid *et al.*[22] explored the consequence of stretching sheet flow with different physical aspects and geometries.

*Corresponding author (E-mail: d11.santosh@yahoo.com)

In the fluid flow problems, usually there are two types of boundary conditions taken, such as no-slip and slip conditions. The no-slip conditions imply that there is no relative motion between fluid and the plate but some surfaces exist where the fluids slip against the sheets. Meanwhile, the slip conditions play a vital role in medical sciences, lubrications, biological liquids and polishing artificial heart valves. Ariel[23], probably, had been the first to find the partial slip effect on an axisymmetric flow. Later on, a second order slip flow model has been developed by Fang *et al.*[24]. Moreover, the flow characteristics with slip condition at the wall have been examined by Khan *et al.*[25], Hayat *et al.*[26], Chaudhary and Choudhary[27], and Yang *et al.*[28].

Continuing to the above mentioned engineering and industrial applications, the target of present illustration is to increase the behavior of heat transfer and describe the nature of slip flow of CNT-water nanofluid along with stretchable plate. The time dependent analysis is created and computational solutions have been achieved by Runge-Kutta method of order four. This analysis concluded that the performance and the efficiency of flow structure can be improved by choosing the appropriate values of the physical parameters. Such study may find application in fire dynamics in insulations and geothermal energy systems etc. There is always a chance of development of some new experimental or numerical methods which can give new height to advanced technology in the fluid flow areas.

2 Problem Formulation

An unsteady boundary layer flow of an incompressible viscous CNT-water nanofluid model near a stretching surface is examined. The impact of slip condition on the surface is assumed. As Fig. 1 a coordinate system is considered in such a way that $x-$axis is measured alongside the plate while $y-$axis is perpendicular to it and fluid flow is defined in the space $y>0$. The velocity at the surface is assumed $u_w=\dfrac{cx}{1-at}$ with the slip velocity $u_{slip}=N_1\nu_f\dfrac{\partial u}{\partial y}$ where c and a are positive constants, t is the time, $N_1=N(1-at)^{1/2}$ is the velocity slip factor, N is the initial value of velocity slip factor, subscript f denotes the thermophysical properties for base fluid, $\nu=\dfrac{\mu}{\rho}$ is the kinematic viscosity, μ is the coefficient of viscosity, ρ is the density and u is the velocity factor in the direction of $x-$axis. Furthermore, the surface temperature $T_w=T_\infty+T_0\dfrac{cx^2}{2\nu_f}\dfrac{1}{(1-at)^{3/2}}$ and the slip temperature $T_{slip}=D_1\dfrac{\partial T}{\partial y}$ are incorporated, where T_∞ is the free stream temperature, T_0 is a measure of the rate of temperature increase along the plate, $D_1=D(1-at)^{1/2}$ is the thermal slip factor, D is the initial value of thermal slip factor and T is the temperature of nanofluid. The basic governing equations after using the boundary layer approximations as (Bansal[29])

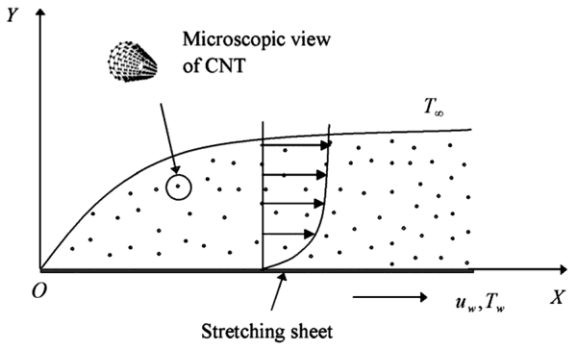

Fig. 1— Flow sketch and coordinate system.

$$\frac{\partial u}{\partial x}+\frac{\partial v}{\partial y}=0 \qquad \ldots (1)$$

$$\frac{\partial u}{\partial t}+u\frac{\partial u}{\partial x}+v\frac{\partial u}{\partial y}=\upsilon_{nf}\frac{\partial^2 u}{\partial y^2} \qquad \ldots (2)$$

$$\frac{\partial T}{\partial t}+u\frac{\partial T}{\partial x}+v\frac{\partial T}{\partial y}=\alpha_{nf}\frac{\partial^2 T}{\partial y^2} \qquad \ldots (3)$$

subjected to the boundary conditions

$$y=0:\ u=u_w+u_{slip},\ v=0,\ T=T_w+T_{slip}$$
$$y\to\infty:\quad u\to 0,\ T\to T_\infty \qquad \ldots (4)$$

where subscript nf indicates the thermophysical properties of nanofluid, v is the velocity factor corresponding to the $y-$axis, $\alpha=\dfrac{\kappa}{\rho C_p}$ is the thermal diffusivity, κ is the thermal conductivity and C_p is the specific heat at constant pressure.

Moreover, thermophysical characteristics of nanofluid, restricted to spherical nanoparticles like coefficient of viscosity, density, thermal conductivity and heat capacitance followed by Khalid *et al.*[30] are given as follows

$$\mu_{nf} = \frac{\mu_f}{(1-\phi)^{5/2}} \quad \ldots (5)$$

$$\rho_{nf} = \left(1-\phi+\phi\frac{\rho_{CNT}}{\rho_f}\right)\rho_f \quad \ldots (6)$$

$$\kappa_{nf} = \frac{1-\phi+2\phi\dfrac{\kappa_{CNT}}{\kappa_{CNT}-\kappa_f}\ln\dfrac{\kappa_{CNT}+\kappa_f}{2\kappa_f}}{1-\phi+2\phi\dfrac{\kappa_f}{\kappa_{CNT}-\kappa_f}\ln\dfrac{\kappa_{CNT}+\kappa_f}{2\kappa_f}}\kappa_f \quad \ldots (7)$$

$$\left(\rho C_p\right)_{nf} = \left[1-\phi+\phi\frac{\left(\rho C_p\right)_{CNT}}{\left(\rho C_p\right)_f}\right]\left(\rho C_p\right)_f \quad \ldots (8)$$

where subscript CNT stands for the physical characteristics for carbon nanotubes and ϕ is the solid volume fraction. Consequently, the values of thermophysical properties of nanofluid are represented by the Table 1 [Khalid *et al.*[30] and Mohammad and Kandasamy[31]].

3 Analysis

The following dimensionless variables are utilized to convert the partial differential equations into a set of ordinary differential equations [Mukhopadhyay and Andersson[32]]

$$\psi = \left(\frac{c\upsilon_f}{1-at}\right)^{1/2} x\, f(\eta),\quad \eta = \left[\frac{c}{\upsilon_f(1-at)}\right]^{1/2} y,\quad T = T_\infty + (T_w - T_\infty)\theta(\eta) \quad \ldots (9)$$

where $\psi(x, y, t)$ is the stream function, which is defined in the usual way as $u = \dfrac{\partial\psi}{\partial y}$ and $v = -\dfrac{\partial\psi}{\partial x}$, and symmetrically satisfy the continuity Eq. (1), $f(\eta)$ is the non-dimensional stream function, η is the similarity variable and $\theta(\eta)$ is the non-dimensional temperature.

Table 1 — Thermophysical characteristics of CNT and water.

Materials	$\rho\ (kgm^{-3})$	$\kappa (Wm^{-1}K^{-1})$	$C_p\ (Jkg^{-1}K^{-1})$
CNT	2600	6600	425
Water	997.1	0.613	4179

Using the mentioned transformations Eq. (9), the momentum and the thermal energy Eqs. (2) and (3) with the associated boundary conditions Eq. (4) have taken the forms

$$f''' + (1-\phi)^{5/2}\left(1-\phi+\phi\frac{\rho_{CNT}}{\rho_f}\right)\left[\left(f-\frac{A}{2}\eta\right)f'' - (f'+A)f'\right] = 0 \quad \ldots (10)$$

$$\frac{\kappa_{nf}}{\kappa_f}\frac{1}{\Pr}\theta'' + \left[1-\phi+\phi\frac{\left(\rho C_p\right)_{CNT}}{\left(\rho C_p\right)_f}\right]\left[\left(f-\frac{A}{2}\eta\right)\theta' - \left(2f'+\frac{3A}{2}\right)\theta\right] = 0 \quad \ldots (11)$$

with the relevant boundary conditions

$$\eta = 0: \quad f = 0,\ f' = 1+\lambda f'',\ \theta = 1+\beta\theta'$$
$$\eta \to \infty: \quad f' \to 0,\ \theta \to 0 \quad \ldots (12)$$

where prime $(')$ mentions the differentiation in terms of η, $A = \dfrac{a}{c}$ is the unsteadiness parameter, $\Pr = \dfrac{\upsilon_f}{\alpha_f}$ is the Prandtl number, $\lambda = N(c\nu_f)^{1/2}$ is the velocity slip parameter and $\beta = D\left(\dfrac{c}{\nu_f}\right)^{1/2}$ is the thermal slip parameter.

4 Physical Quantities

The important quantities of physical interest in this study are the local skin friction coefficient C_f and the local Nusselt number Nu_x, which are given by

$$C_f = \frac{\mu_{nf}\left(\dfrac{\partial u}{\partial y}\right)_{y=0}}{\dfrac{\rho_f u_w^{\,2}}{2}},\quad Nu_x = -\frac{\kappa_{nf}\, x\left(\dfrac{\partial T}{\partial y}\right)_{y=0}}{\kappa_f(T_w - T_\infty)} \quad \ldots (13)$$

By substituting the dimensionless variables Eq. (9), the physical quantities Eq. (13) can be expressed in the following forms

$$\mathrm{Re}_x^{1/2} C_f = \frac{2}{(1-\phi)^{5/2}} f''(0), \quad \frac{1}{\mathrm{Re}_x^{1/2}} Nu_x = -\frac{\kappa_{nf}}{\kappa_f}\theta'(0) \qquad \ldots (14)$$

where $\mathrm{Re}_x = \frac{u_w x}{\upsilon_f}$ is the local Reynolds number.

5 Solution Methodology

Numerical values of the Eqs. (10) and (11) with the associated boundary conditions Eq. (12) are computed by applying the perturbation technique. Introducing the power series in terms of small unsteadiness parameter A as follows

$$f(\eta) = \sum_{i=0}^{\infty} A^i f_i(\eta) \qquad \ldots (15)$$

$$\theta(\eta) = \sum_{j=0}^{\infty} A^j \theta_j(\eta) \qquad \ldots (16)$$

Substituting the Eqs. (15) and (16) and its derivative in the governing Eqs. (10) to (12) and then equating the coefficients of like power of A

$$f_0''' + (1-\phi)^{5/2}\left(1-\phi+\phi\frac{\rho_{CNT}}{\rho_f}\right)\left(f_0 f_0'' - f_0'^2\right) = 0 \qquad \ldots (17)$$

$$\frac{\kappa_{nf}}{\kappa_f}\frac{1}{\mathrm{Pr}}\theta_0'' + \left[1-\phi+\phi\frac{(\rho C_p)_{CNT}}{(\rho C_p)_f}\right]\left(f_0\theta_0' - 2f_0'\theta_0\right) = 0 \qquad \ldots (18)$$

$$f_1''' + (1-\phi)^{5/2}\left(1-\phi+\phi\frac{\rho_{CNT}}{\rho_f}\right)\left(f_0 f_1'' - 2f_0' f_1' + f_0'' f_1\right) = (1-\phi)^{5/2}\left(1-\phi+\phi\frac{\rho_{CNT}}{\rho_f}\right)\left(\frac{1}{2}\eta f_0'' + f_0'\right) \qquad \ldots (19)$$

$$\frac{\kappa_{nf}}{\kappa_f}\frac{1}{\mathrm{Pr}}\theta_1'' + \left[1-\phi+\phi\frac{(\rho C_p)_{CNT}}{(\rho C_p)_f}\right]\left(f_0\theta_1' - 2f_0'\theta_1\right) = \left[1-\phi+\phi\frac{(\rho C_p)_{CNT}}{(\rho C_p)_f}\right]\left[\left(-f_1+\frac{1}{2}\eta\right)\theta_0' + \left(2f_1'+\frac{3}{2}\right)\theta_0\right] \qquad \ldots (20)$$

$$f_2''' + (1-\phi)^{5/2}\left(1-\phi+\phi\frac{\rho_{CNT}}{\rho_f}\right)\left(f_0 f_2'' - 2f_0' f_2' + f_0'' f_2\right) = (1-\phi)^{5/2}\left(1-\phi+\phi\frac{\rho_{CNT}}{\rho_f}\right)\left[\left(-f_1+\frac{1}{2}\eta\right)f_1'' + (f_1'+1)f_1'\right] \qquad \ldots (21)$$

$$\frac{\kappa_{nf}}{\kappa_f}\frac{1}{\mathrm{Pr}}\theta_2'' + \left[1-\phi+\phi\frac{(\rho C_p)_{CNT}}{(\rho C_p)_f}\right]\left(f_0\theta_2' - 2f_0'\theta_2\right) = \left[1-\phi+\phi\frac{(\rho C_p)_{CNT}}{(\rho C_p)_f}\right]\left[\left(-f_1+\frac{1}{2}\eta\right)\theta_1' + \left(2f_1'+\frac{3}{2}\right)\theta_1 - f_2\theta_0' + 2f_2'\theta_0\right] \qquad \ldots (22)$$

with the boundary conditions

$$\eta = 0: \quad f_i = 0,\ f_0' = 1+\lambda f_0'',\ f_j' = \lambda f_j'',\ \theta_0 = 1+\beta\theta_0',\ \theta_j = \beta\theta_j'$$
$$\eta \to \infty: \quad f_i' \to 0,\ \theta_i \to 0 \qquad i \geq 0,\ j > 0 \qquad \ldots (23)$$

The fourth order Runge-Kutta method is applied for the numerical solution of the ordinary differential Eqs. (17) to (22) with boundary conditions Eq. (23), which employed step size 0.001 to obtain the solution. Above procedure is repeated until the results are correct up to the pertinent accuracy of 10^{-7} level are found.

6 Validation of Results

For the validation of numerical technique, the values of the heat flux are carried and compared with previously reported data. These comparisons are presented in Table 2, which declares the comparison of the heat transfer rate versus Prandtl number. From this table, it can be observed that the present results are in good agreement with the numerical values found by Mukhopadhyay and Andersson[32].

Table 2 — Comparision for the values of $-\theta'(0)$ with the previously published results when $\lambda = \phi = A = \beta = 0$ and $f''(0) = -1.000483$.

Pr	Mukhopadhyay and Andersson[32]	Present Results
0.72	1.08855	1.0900635
1.00	1.33334	1.3333439
3.00	2.50971	2.5095146

7 Discussion of Numerical Results

In this section, figures are given to discuss the significance of the velocity slip parameter λ, the solid volume fraction ϕ, the unsteadiness parameter A and the thermal slip parameter β on the velocity $f'(\eta)$ and the temperature $\theta(\eta)$ profiles, while table represents the numerical data of the surface shear stress $f''(0)$ and the surface heat flux $\theta'(0)$ for the impacts of specified parameters. To find the effect of anyone of physical parameters, the other remaining parameters are taken as fixed value.

Figures 2 and 3 depict the effects of the velocity slip parameter λ on the velocity $f'(\eta)$ and the temperature $\theta(\eta)$ fields respectively. The momentum boundary layer as well as the thermal boundary layer increases when λ develops, but a reverse impact can be seen in momentum boundary layer for $\eta < 2.75$. The central reason for increment in velocity and temperature of the fluid is that the extraction in stretching sheet is partially communicated in the liquid over the slip condition and heat transfer from heated surface into the adjacent fluid is in more quantity.

Fluctuations in the dimensionless velocity $f'(\eta)$ and the temperature $\theta(\eta)$ for the changes in the solid volume fraction ϕ are conferred in Figs 4 and 5, respectively. These figures elucidate that the fluid flow and the fluid temperature enhance along with the booming values of ϕ. This is because nanofluid has higher viscosity along with the rising solid volume fraction which leads to nanofluid velocity falls, while the nanofluid velocity develops for the slip condition. Moreover, an increment in the solid volume fraction causes enlargement in the thermal conductivity, so thermal boundary layer thickness increases.

Figures 6 and 7 illustrate the behavior of the velocity $f'(\eta)$ and the temperature $\theta(\eta)$ distributions with the influences of the unsteadiness parameter A respectively. From these figures it can be observed that an increment in A tends to reduce the fluid velocity as well as the fluid temperature while opposite phenomenon can be noted in velocity for $\eta > 2.75$. Physically, along with the increment in the unsteadiness parameter, the heat declines at the wall, which imply the depreciation in the velocity and the temperature.

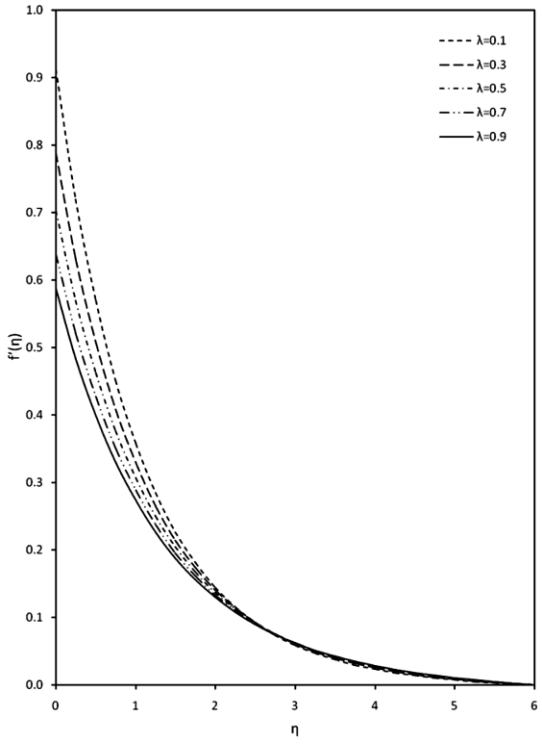

Fig. 2 — Behavior of dimensionless velocity for different λ with $\phi = 0.08$ and $A = 0.1$.

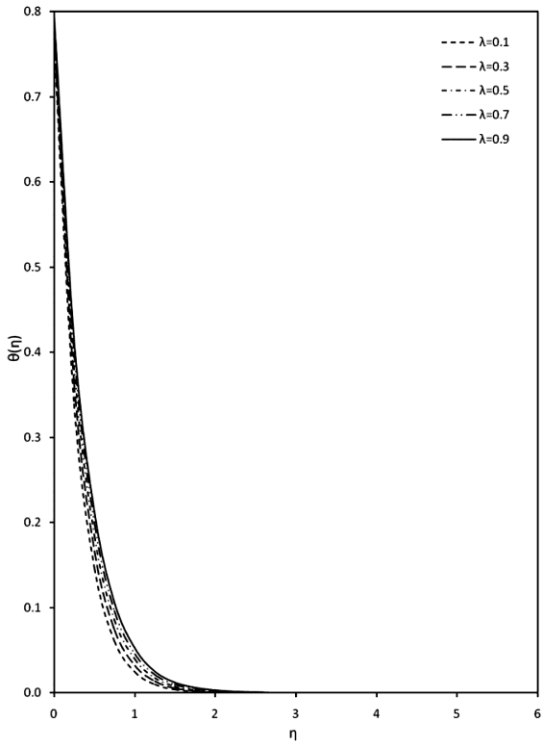

Fig. 3 — Behavior of dimensionless temperature for different λ with $\phi = 0.08$, $A = 0.1$, $\beta = 0.1$ and $\mathrm{Pr} = 6.2$.

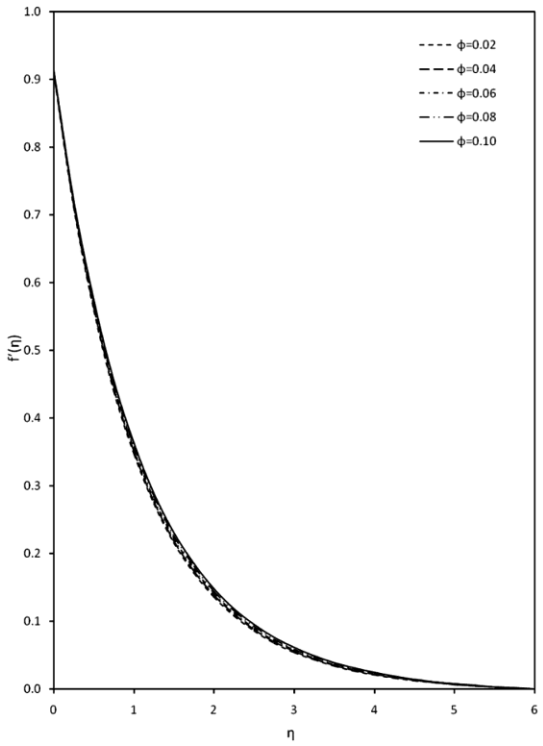

Fig. 4 — Behavior of dimensionless velocity for different ϕ with $\lambda = 0.1$ and $A = 0.1$.

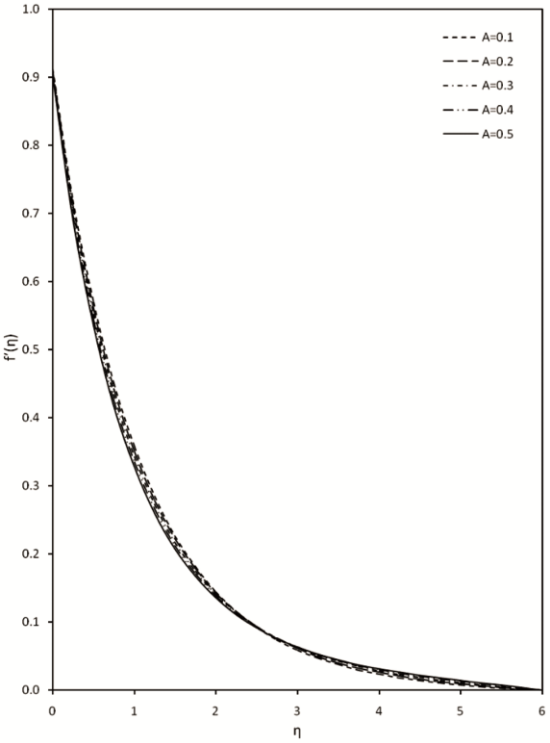

Fig. 6 — Behavior of dimensionless velocity for different A with $\lambda = 0.1$ and $\phi = 0.08$.

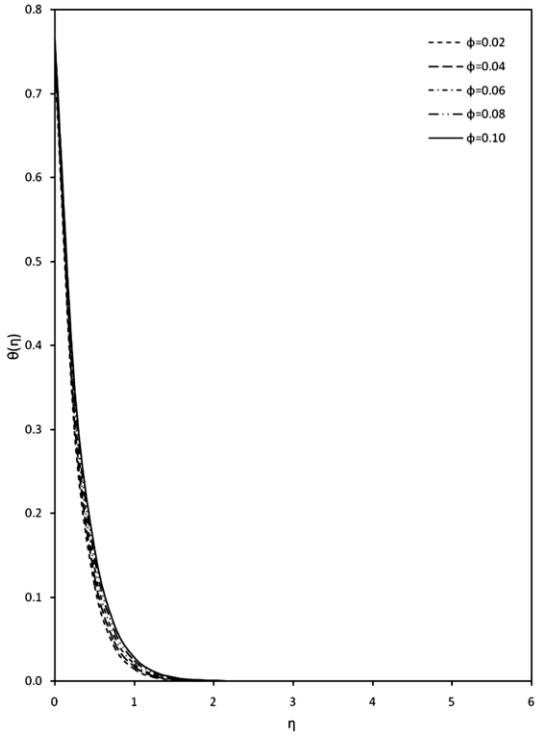

Fig. 5 — Behavior of dimensionless temperature for different ϕ with $\lambda = 0.1$, $A = 0.1$, $\beta = 0.1$ and $\mathrm{Pr} = 6.2$.

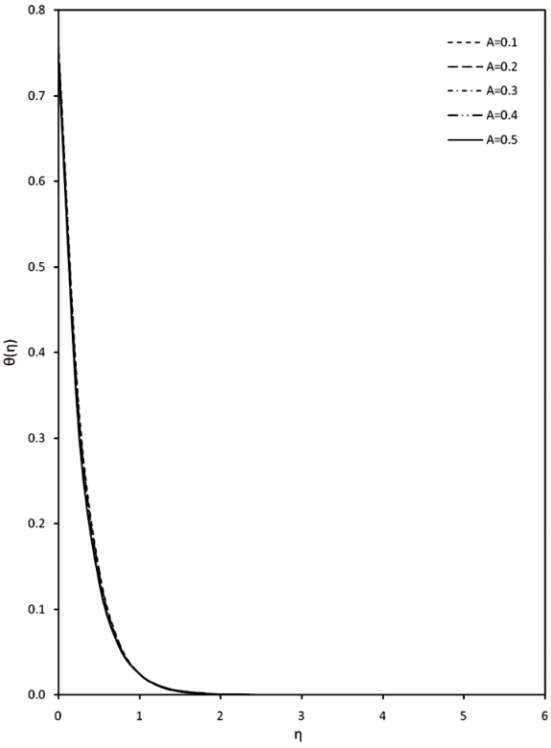

Fig. 7 — Behavior of dimensionless temperature for different A with $\lambda = 0.1$, $\phi = 0.08$, $\beta = 0.1$ and $\mathrm{Pr} = 6.2$.

The behavior of the thermal slip parameter β on the temperature of fluid $\theta(\eta)$ is demonstrated in Fig. 8. One can observe from this figure that the enlarging value of β declines the thermal boundary layer. This is because of the less amount of heat is transferred from the plate to the fluid as the thermal slip parameter step-up.

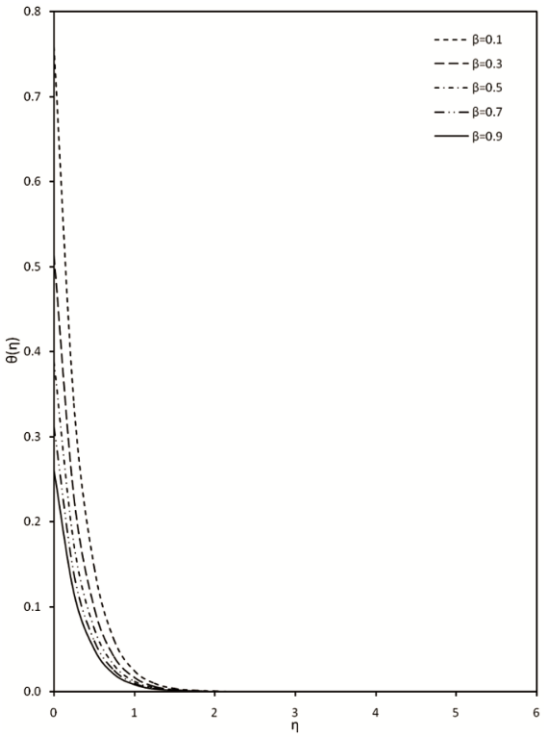

Fig. 8 — Behavior of dimensionless temperature for different β with $\lambda = 0.1$, $\phi = 0.08$, $A = 0.1$ and $\Pr = 6.2$.

Table 3 — Numerical data of $f''(0)$ and $\theta'(0)$ for several values of specified parameters with $\Pr = 6.2$.

λ	ϕ	A	β	$-f''(0)$	$-\theta'(0)$
0.1	0.08	0.1	0.1	0.8673166	2.3884392
0.3				0.7013914	2.2661651
0.5				0.5930364	2.1730953
0.7				0.5158499	2.0981672
0.9				0.4576844	2.0356264
0.1	0.02			0.8936792	2.5998101
	0.04			0.8855847	2.5272450
	0.06			0.8767897	2.4568361
	0.10			0.8571861	2.3219240
	0.08	0.2		0.8943876	2.4354485
		0.3		0.9210110	2.4811471
		0.4		0.9471189	2.5256039
		0.5		0.9726596	2.5688782
		0.1	0.3	0.8673166	1.6163354
			0.5		1.2214733
			0.7		0.9816592
			0.9		0.8205576

Table 3 shows the numerical values of the surface shear stress $f''(0)$ and the rate of heat transfer $\theta'(0)$ for different controlling parameters respectively. This table concludes that the local skin friction coefficient and the local Nusselt number enhances for increasing values of λ and ϕ, while an opposite reaction can be seen for rising values of A. Further, an enlargement in β leads to an increase in the surface heat flux. Furthermore, for effects of all considering parameters, the negative values of the wall shear stress and the heat flux imply that fluid yields a drag force by the surface and there is a heat flow to the surface respectively.

8 Conclusions

Slip effect on unsteady CNT-water nanofluid flow along with stretching sheet is studied in this problem. The governing partial differential equations are converted into a set of ordinary differential equations by similarity transformation. Perturbation technique along with Runge-Kutta fourth order method is used to obtain the numerical solutions of the resulting system. The following findings are established

(i) The velocity, temperature, the surface shear stress and the surface heat flux increase as the velocity slip parameter and the solid volume fraction rise, while opposite phenomenon occurs in the velocity profile for $\eta < 2.75$ along with the increment in the velocity slip parameter.

(ii) An enhancement in the unsteadiness parameter leads to decrease the dimensionless velocity, temperature, the local skin friction and the local Nusselt number, whereas the velocity distribution rises for $\eta > 2.75$.

(iii) In the presence of the booming thermal slip parameter, the thermal boundary layer decreases and the rate of heat transfer enhances.

References

1 Elbashbeshy E M A & Bazid M A A, *Heat Mass Transf*, 41 (2004) 1.
2 Liao S, *Commun Nonlinear Sci Numer Simul*, 11 (2006) 326.
3 Jat R N & Chaudhary S, *Il Nuovo Cimento*, 124 B (2009) 53.
4 Hayat T & Nawaz M, *J Taiwan Inst Chem Eng*, 42 (2011) 41.
5 Rashad A M, *J Egypt Math Soc*, 22 (2014) 134.
6 Khan M & Azam M, *Results Phys*, 6 (2016) 1168.

7 Chaudhary S & Choudhary M K, *Indian J Pure Appl Phys*, 55 (2017) 864.
8 Dholey S, *Eur J Mech B Fluids*, 70 (2018) 102.
9 Moshkin N P, Pukhnachev V V & Bozhkov Y D, *Int J Non Linear Mech*, 116 (2019) 32.
10 Choi S U S, *Publ Fed*, 231ASME (1995) 99.
11 Sheikholeslami M & Ganji DD, *Powder Technol*, 235 (2013) 873.
12 Chen Cha'o-Kuang, Chen Bo-Shiuan & Liu Chin-Chia, *Int J Heat Mass Transf*, 91 (2015) 1026.
13 Sheikholeslami M & Rokni H B, *Chinese J Phys*, 55 (2017) 1352.
14 Ahmed Z & Nadeem S, *Phys Scr*, 94 (2019) 105203.
15 Chaudhary S & Kanika KM, *Int J Comput Math*, 97 (2020) 943.
16 Uddin M J, Kabir M N, Alginahi Y & Bég O A, *Proc Inst Mech Eng, Part C: J Mech Eng Sci*, 233 (2019) 6910.
17 Ishak A, Jafar K, Nazar R & Pop I, *Phys A: Statist Mech Appl*, 388 (2009) 3377.
18 Tamizharasi R & Kumaran V, *Commun Nonlinear Sci Numer Simul*, 16 (2011) 4671.
19 Chaudhary S, Choudhary M K & Sharma R, *Meccanica*, 50 (2015) 1977.
20 Babu M J & Sandeep N, *Adv Powder Technol*, 27 (2016) 2039.
21 Liu L & Liu F, *Appl Math Lett*, 79 (2018) 92.
22 Hamid M, Usman M, Khan Z H, Ahmad R & Wang W, *Phys Lett A*, 383 (2019) 2400.
23 Ariel P D, *Comput Math Appl*, 54 (2007) 1169.
24 Fang T, Yao S, Zhang J & Aziz A, *Commun Nonlinear Sci Numer Simul*, 15 (2010) 1837.
25 Khan WA, Uddin MJ & Ismail AIM, *Plos One* 8 (2013) e54024.
26 Hayat T, Shafiq A, Alsaedi A & Shahzad S A, *Appl Math Mech*, 37 (2016) 193.
27 Chaudhary S & Choudhary M K, *Therm Sci*, 22 (2018) 797.
28 Yang L, Yu Y, Pei H, Gao Y & Hou G, *Chem Eng Sci*, 202 (2019) 105.
29 Bansal J L, Magnetohydrodynamics of viscous fluids. *Jaipur Pub House, India* (1994).
30 Khalid A, Khan I, Khan A, Shafie S & Tlili I, *Therm Eng*, 12 (2018) 374.
31 Mohammad R & Kandasamy R, *J Mol Liq*, 237 (2017) 54.
32 Mukhopadhyay S & Andersson H I, *Heat Mass Transf*, 45 (2009) 1447.